Synthesis and evaluation of radioiodinated 1-(2-[5-(2-methoxyethoxy)-1H-benzo[d]imidazol-1-yl]quinolin-8-yl)piperidin-4-amine derivatives for platelet-derived growth factor receptor β (PDGFRβ) imaging

doi: 10.1016/j.bmc.2017.08.025

Synthesis and evaluation of radioiodinated 1-{2-[5-(2-methoxyethoxy)-1*H*-benzo[*d*]imidazol-1-yl]quinolin-8-yl}piperidin-4-amine derivatives for platelet-derived growth factor receptor β (PDGFRβ) imaging

Nurmaya Effendi[a,b], Kazuma Ogawa[a,c*], Kenji Mishiro[c], Takeshi Takarada[d], Daisuke Yamada[d,f], Yoji Kitamura[e], Kazuhiro Shiba[e], Takehiko Maeda[f], Akira Odani[a]

[a]*Kanazawa University, Graduate School of Pharmaceutical Sciences, Kakuma-machi, Kanazawa, Ishikawa 920-1192, Japan;*

[b]*Universitas Muslim Indonesia, Faculty of Pharmacy, Urip Sumiharjo KM. 10, Makassar 90-231, Indonesia;*

[c]*Kanazawa University, Institute for Frontier Science Initiative, Kakuma-machi, Kanazawa, Ishikawa 920-1192, Japan;*

[d]*Okayama University, Graduate School of Medicine, Department of Regenerative Science, Dentistry and Pharmaceutical Sciences, Okayama, 700-8558, Japan;*

[e]*Kanazawa University, Advanced Science Research Centre, Takara-machi, Kanazawa, Ishikawa 920-8640, Japan;*

[f]*Niigata University of Pharmacy and Applied Sciences, Division of Pharmacology, 265-1 Higashijima, Akiha-ku, Niigata-shi, Niigata-ken, 956-8603, Japan.*

***Corresponding Author**

Kazuma Ogawa Tel.: 81-76-234-4460; fax: 81-76-234-4459;

E-mail: kogawa@p.kanazawa-u.ac.jp

Running Title: PDGFRβ imaging agent

Word Count of this manuscript: 5125 words

Conflict of interest: The authors have declared that no conflict of interest.

Financial support: This work was supported in part by Grants-in-Aid for Scientific Research (16H01332, 16KT0192) from the Ministry of Education, Culture, Sports, Science and Technology, Japan.

Abstract

Platelet-derived growth factor receptor β (PDGFRβ) is a transmembrane tyrosine kinase receptor and it is upregulated in various malignant tumors. Radiolabeled PDGFRβ inhibitors can be a convenient tool for the imaging of tumors overexpressing PDGFRβ. In this study, [^{125}I]-1-{5-iodo-2-[5-(2-methoxyethoxy)-1*H*-benzo[*d*]imidazol-1-yl]quinoline-8-yl}piperidin-4-amine ([^{125}I]IIQP) and [^{125}I]-*N*-3-iodobenzoyl-1-{2-[5-(2-methoxyethoxy)-1*H*-benzo[*d*]imidazol-1-yl]quinolin-8-yl}-piperidin-4-amine ([^{125}I]IB-IQP) were designed and synthesized, and their potential as PDGFRβ imaging agents was evaluated. In cellular uptake experiments, [^{125}I]IIQP and [^{125}I]IB-IQP showed higher uptake by PDGFRβ-positive cells than by PDGFRβ-negative cells, and the uptake in PDGFRβ-positive cells was inhibited by co-culture with PDGFRβ ligands. The biodistribution of both radiotracers in normal mice exhibited hepatobiliary excretion as the main route. In mice inoculated with BxPC3-luc (PDGFRβ-positive), the tumor uptake of radioactivity at 1 h after the injection of [^{125}I]IIQP was significantly higher than that after the injection of [^{125}I]IB-IQP. These results indicated that [^{125}I]IIQP can be a suitable PDGFRβ imaging agent. However, further modification of its structure will be required to obtain a more appropriate PDGFRβ-targeted imaging agent with a higher signal / noise ratio.

Keywords: radiotracer, molecular imaging, PDGFRβ, tyrosine kinase inhibitor

1. Introduction

PDGFRβ belongs to a subfamily of receptor tyrosine kinases (RTKs). It possesses an outer membrane with a PDGF ligand binding site and an inner membrane tyrosine kinase (TK) domain with an adenosine triphosphate (ATP) binding site.[1] Binding of PDGF ligands to the extracellular binding domain triggers PDGFRβ dimerization, thus inducing phosphorylation of its intracellular regions due to an activated ATP-binding domain. This is followed by the activation of signaling pathways that regulate important cellular functions.[2] The expression of PDGFRβ is highly restricted in most normal cells; however, upregulation of PDGFRβ in numerous human tumors and its relationship with tumor progression features such as cell migration, metastasis, angiogenesis, and proliferation, have been reported.[3-5] Therefore, PDGFRβ can be an attractive target not only for cancer therapy but also for developing tumor-imaging agents.[6-8]

Nuclear medicine has been a revolutionary invention in the field of diagnostic imaging because it is noninvasive and facilitates continuous monitoring of disease progression or treatment response.[9,10] Moreover, the imaging modalities in nuclear medicine, such as single photon emission computed tomography (SPECT) and positron emission tomography (PET) can quantify receptor density and molecular target expression in patients, thus becoming a useful tool in drug development.[10-12] Previous studies have reported imaging agents, including radiolabeled protein,[13,14] aptamer,[15] affibody molecules,[16,17] and peptide[18,19] that target the extracellular parts of PDGFRβ. Although the imaging of intracellular parts of PDGFRβ, particularly its ATP-binding site, has hardly been reported,[8] the ATP-binding is very important for

following signal transductions and growth of cancer cells. Therefore, the ATP-binding site can be a target for TK inhibitors (TKIs). Meanwhile, mutations of the ATP-binding site have frequently been found[20,21]. The mutation status often affects therapeutic effects of TKIs. Thus, the information of the ATP-binding site, containing the mutation status, is useful for the prediction of therapeutic effects of TKIs. Other radiolabeled TK inhibitors (TKIs)[22-26] and their potential advantages, such as assessment of drug sensitivity[20], mutation status[21], and usefulness in drug screening[11,27,28] have been demonstrated.

1-{2-[5-(2-Methoxyethoxy)-1*H*-benzo[*d*]imidazol-1-yl]quinolin-8-yl}piperidin-4-amine (CP-673451, IQP) (Figure 1) is a highly selective benzimidazole inhibitor of PDGFRβ (IC_{50} = 1 nM) over PDGFRα (IC_{50} = 10 nM). Importantly, it is 1,000 times selective compared with many other RTKs. It competitively inhibits ATP-binding to the ATP-binding site of PDGFRβ and blocks phosphorylation.[29,30] High binding affinity and high selectivity to the molecular target are important for a lead compound of imaging probes. IQP can be an attractive compound in an attempt to image the ATP binding site of PDGFRβ. Therefore, we speculated that radiolabeled IQP derivatives that bind the ATP-binding site may be useful imaging probes.

To develop novel radiolabeled molecular probes for PDGFRβ imaging, we chose radioiodine as a radionuclide in this study because ^{123}I ($t_{1/2}$ = 13.2 h) and ^{124}I ($t_{1/2}$ = 4.2 d) are useful radionuclides for SPECT and PET, respectively. We did not have sufficient information about the introduction of radioiodine into IQP structure to retain high affinity for PDGFRβ. To evaluate the feasibility of IQP derivatives as

PDGFRβ imaging probes, we designed and synthesized two different types of iodine labeled IQP, 1-{5-iodo-2-[5-(2-methoxyethoxy)-1*H*-benzo[*d*]imidazol-1-yl]quinolin-8-yl}piperidin-4-amine (IIQP) and *N*-3-iodobenzoyl-1-{2-[5-(2-methoxyethoxy)-1*H*-benzo[*d*]imidazol-1-yl]-quinolin-8-yl}-piperidin-4-amine (IB-IQP). In IIQP, iodine was directly introduced to C-5 of the quinoline group of IQP because it is a reactive site for halogenation of IQP. In IB-IQP, iodine was indirectly introduced by conjugation of 3-iodo benzoyl group using SIB (*N*-succinimidyl-3-iodobenzoate) with the primary amine group of IQP. We then examined the binding affinities of two derivatives for PDGFRβs. Subsequently, radiotracers [^{125}I]IIQP and [^{125}I]IB-IQP (Figure 1) were synthesized and evaluated *in vitro* and *in vivo* to investigate their usefulness as PDGFRβ imaging agents. Although we are interested in developing imaging probes for SPECT and PET, ^{125}I was used as an alternative radionuclide in these initial studies because of its long half-life ($t_{1/2}$ = 59.4 d).

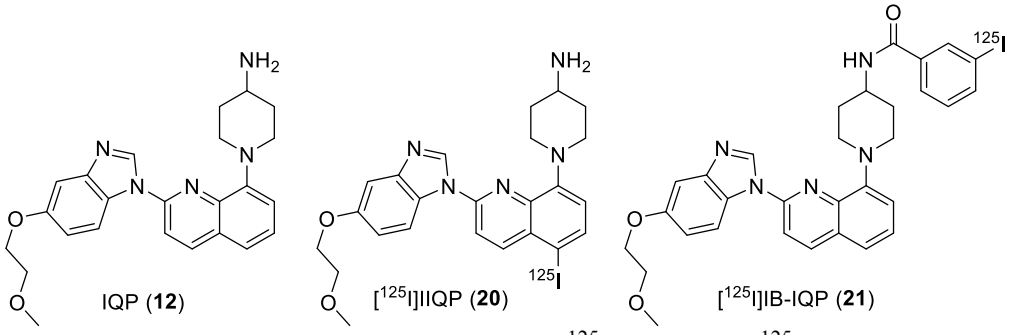

Figure 1. Chemical structures of IQP, [^{125}I]IIQP, and [^{125}I]IB-IQP.

2. Material and methods

2.1. General

Commercial reagents and solvents were purchased from Sigma-Aldrich (St. Louis, MO, USA), Wako Pure Chemical Industries (Osaka, Japan), Nacalai Tesque,

Inc., (Kyoto, Japan), Tokyo Chemical Industry, Co., Ltd., (Tokyo, Japan) and Kanto Chemical, Co., Inc. (Tokyo, Japan) and used without further purification unless otherwise stated.

[^{125}I]Sodium iodide (644 GBq/mg) was purchased from Perkin Elmer (Waltham, MA, USA). The radioactivity was measured by an Auto Gamma System ARC-7010B (Hitachi, Ltd., Tokyo, Japan).

Bicinchoninic Acid (BCA) Protein Assay Kit and Cell Counting Kit (CCK) were purchased from Nacalai Tesque, Inc. and Dojindo (Kumamoto, Japan), respectively. Recombinant murine platelet-derived growth factor-BB (PDGF-BB) was purchased from PeproTech (Rocky Hill, NJ, USA). TR-PCT1 rodent brain pericyte cell line was a generous gift from Dr. Emi Nakashima (Keio University, Tokyo, Japan),[31] MCF7 breast cancer cell lines were purchased from DS Pharma Biomedical (Osaka, Japan), and BxPC3-luc pancreatic cell line was purchased from JCRB Cell Bank (Ibaraki, Japan).

Proton and carbon nuclear magnetic resonance (^{1}H-NMR and ^{13}C-NMR) spectra were obtained with JEOL JNM-ECS400 (JEOL Ltd, Tokyo, Japan). Direct analysis in real time mass spectra (DART-MS) and Electrospray ionization mass spectra (ESI-MS) were obtained with JEOL JMS-T100TD (JEOL Ltd). Purification were conducted using reversed-phase high-performance liquid chromatography (RP-HPLC) system. TLC analysis were performed with silica plates (Art 5553, Merck, Darmstadt, Germany). Optical density in WST-8 assay was obtained using Infinite® F200 Pro microplate reader (TECAN, Männedorf, Switzerland).

2.2. *Synthesis of reference compounds and precursors*

Intermediate and reference compounds, IQP, ATE, and SIB, were synthesized according to the reported studies, with a slight modification.[32-37] Detailed procedures were shown in the Supporting Information.

*2.2.1. 1-{5-Iodo-2-[5-(2-methoxyethoxy)-1H-benzo[d]imidazol-1-yl]quinolin-8-yl}piperidin-4-amine (IIQP) (**13**)*

A mixture of *N*-chlorosuccinimide (NCS) (80 mg, 0.6 mmol, 1.2 eq.) and sodium iodide (NaI) (90 mg, 0.6 mmol, 1.2 eq.) in acetic acid (5 mL) was added to **12** (209 mg, 0.5 mmol, 1.0 eq.) in acetic acid (5 mL) and the mixture was stirred at 50 °C for 18 h under nitrogen atmosphere. After adjusting pH to 9.0 using saturated aqueous sodium bicarbonate ($NaHCO_3$), the reaction mixture was extracted with dichloromethane (3 x 30 mL). The organic layer was dried over sodium sulfate, filtered, and concentrated under reduced pressure. The crude product was purified by column chromatography on silica gel (chloroform/methanol = 50/1) to afford **13** (217 mg, 80%) as a pale yellow solid. ^{1}H NMR (400 MHz, $CDCl_3$): δ 1.76 – 1.85 (2H, m), 2.01 – 2.10 (2H, m), 2.85 – 2.96 (3H, m), 3.50 (3H, s), 3.82 – 3.84 (2H, m), 3.99 (2H, br d), 4.23 – 4.25 (2H, m), 7.00 (1H, d, *J* = 8.0 Hz), 7.26 (1H, dd, *J* = 11.2, 2.0 Hz), 7.38 (1H, d, *J* = 2.0 Hz), 7.74 (1H, d, *J* = 9.2 Hz), 7.98 (1H, d, *J* = 8.0 Hz), 8.39 (1H, d, *J* = 9.2 Hz), 8.56 (1H, d, *J* = 9.2 Hz), 8.68 (1H, s). ^{13}C NMR (100 MHz, $CDCl_3$): δ 156.05, 150.46, 147.08, 145.51, 144.70, 142.19, 141.34, 137.42, 129.16, 126.68, 119.56, 114.91, 114.35, 113.68, 103.52, 88.63, 71.08, 67.77, 59.26, 51.44 (2C), 48.73,

36.28 (2C). HRMS (ESI+) calcd for $C_{24}H_{27}IN_5O_2$ [M+H$^+$]: *m/z* = 544.1204, found 544.1166.

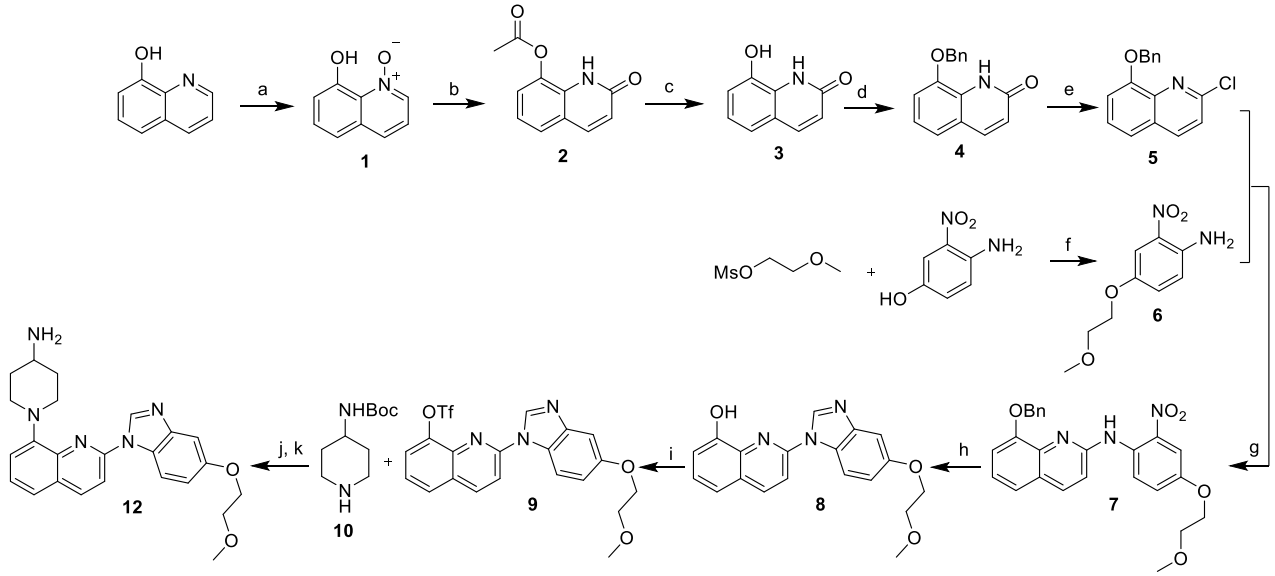

Scheme 1. Synthesis of reference compound IQP (a) sodium tungstate dihydrate, hydrogen peroxide, 75 °C, 5 h (b) acetic anhydrate, 100 °C, 7.5 h (c) HCl, 95 °C, 2 h (d) benzyl bromide, potassium carbonate, reflux, 6 h (e) $POCl_3$, reflux, 16 h (f) cesium carbonate, reflux, 3 d (g) palladium acetate, DIPHOS, cesium carbonate, phenyl boronic acid, 115 °C, 3 d (h) (i) palladium chloride, TEA, formic acid, 65 °C, 2 h (ii) formamidine acetate, reflux, overnight (i) *N*-phenyl-bis(trifluoromethanesulfonimide), room temperature, 2 d (j) cesium carbonate, *rac*-BINAP, tris(dibenzylideneacetone)dipalladium(0), reflux, 3 d (k) TFA, room temperature, 15 min.

*2.2.2. tert-Butyl (1-{5-iodo-2-[5-(2-methoxyethoxy)-1H-benzo[d]imidazol-1-yl]quinolin-8-yl}piperidin-4-yl)carbamate (**14**)*

A mixture of **13** (100 mg, 0.2 mmol, 1.0 eq.), triethylamine (TEA) (56 µL, 0.4 mmol, 2.0 eq.) and di-*tert*-butyl dicarbonate (Boc_2O) (109 mg, 0.5 mmol, 2.5 eq.) in dry dichloromethane (2 mL) was stirred at room temperature for 3 days under nitrogen atmosphere. The reaction mixture was diluted with dichloromethane and washed successively with saturated aqueous $NaHCO_3$ and brine. The organic layer was dried over sodium sulfate, filtered, and concentrated under reduced pressure to afford **14** (100 mg) as a pale yellow solid. The product was used in the following reaction without further purification.

*2.2.3. tert-Butyl (1-{2-[5-(2-methoxyethoxy)-1H-benzo[d]imidazol-1-yl]-5-(tributylstannyl)quinolin-8-yl}piperidin-4-yl)carbamate (tin-IQP) (**15**)*

A mixture of **14** (47 mg, 72.3 µmol, 1.0 eq.), hexabutyldistannane (73 µL, 144.6 µmol, 2.0 eq.), and tetrakis(triphenylphosphine)palladium(0) $Pd[P(C_6H_5)_3]_4$ (4 mg, 3.6 µmol, 5% eq.) in dry toluene (2 mL) was refluxed for 24 h under nitrogen atmosphere. After removing the catalyst by filtration through a pad of Celite® and washing with toluene, the filtrate was concentrated under reduced pressure and purified by HPLC with mobile phase system methanol (A) (with 0.05% TEA) and water (B) (with 0.05% TEA), A : 97.5 – 100%, 20 min using $5C_{18}$ MSII (10ID x 250 mm) column, flow rate 4 mL/min, to afford **15** (28 mg, 48%) as a pale yellow solid. ^{1}H NMR (400 MHz, DMSO-d_6): δ 0.82 – 0.86 (9H, m), 1.11 – 1.21 (6H, m), 1.26 – 1.35 (6H, m), 1.43 (9H, s), 1.47 – 1.59 (6 H, m), 1.83 – 1.88 (4H, m), 2.74 – 2.79 (2H, m), 3.35 (3H, s), 3.46 (1H, br s), 3.72 – 3.74 (2H, m), 3.78 (2H, br d), 4.19 – 4.21 (2H, m), 7.32 (1H, d, J = 7.2 Hz), 7.34 (1H, s), 7.38 (1H, d, J = 8.8 Hz), 7.57 (1H, d, J = 7.6 Hz), 8.17 – 8.23 (2H, m), 8.93 (1H, d, J = 8.8 Hz), 9.16 (1H, s). ^{13}C NMR (100 MHz, $CDCl_3$): δ 155.66, 154.99, 149.57, 146.49, 145.02, 142.18, 141.49, 141.45, 135.50, 134.54, 132.47, 126.25, 118.10, 116.49, 114.49, 112.23, 102.50, 77.51, 70.53, 67.21, 58.19, 51.30 (2C), 47.61, 32.67 (2C), 28.69 (3C), 28.32 (3C), 26.66 (3C), 13.52 (3C), 10.01 (3C). HRMS (ESI+), calcd for $C_{41}H_{62}N_5O_4Sn$ $[M+H^+]$: *m/z* = 808.3818, found 808.3846.

*2.2.4. N-3-iodobenzoyl-1-{2-[5-(2-methoxyethoxy)-1H-benzo[d]imidazol-1-yl]-quinolin-8-yl}-piperidin-4-amine (IB-IQP) (**18**)*

A mixture of **12** (12 mg, 30.0 µmol, 1.0 eq.), *N,N*-diisopropylethylamine (DIPEA) (6 µL, 33.0 µmol, 1.1 eq.), and **17** (11 mg, 33.0 µmol, 1.1 eq.) in dry dichloromethane (1 mL) was stirred at 50 °C for 2 h under nitrogen atmosphere. After completion of the reaction, the reaction mixture was diluted with dichloromethane and washed with water. The organic layer was dried over sodium sulfate, filtered, and concentrated under reduced pressure. The crude product was purified by column chromatography on silica gel (chloroform/methanol = 100/1) to afford **18** (15 mg, 77%) as a colorless solid. ^{1}H-NMR (400 MHz, DMSO-d_6): δ 2.01 – 2.06 (4H, m), 2.86 – 2.91 (2H, m), 3.32 (3H, s), 3.71 – 3.73 (2H, m), 3.87 (2H, br d), 4.02 (1H, br s), 4.19 – 4.21 (2H, m), 7.31 – 7.38 (4H, m), 7.52 (1H, t, J = 8.0 Hz), 7.65 (1H, d, J = 8.4 Hz), 7.92 (2H, t, J = 8.0 Hz), 8.19 (1H, d, J = 8.8 Hz), 8.24 (1H, s), 8.56 (1H, d, J = 8.4 Hz), 8.64 (1H, d, J = 8.0 Hz), 8.95 (1H, d, J = 8.8 Hz), 9.19 (1H, s). ^{13}C NMR (100 MHz, $CDCl_3$): δ 164.41, 155.56, 149.04, 146.97, 145.08, 142.42, 140.50, 140.34, 139.66, 136.95, 135.67, 130.48, 127.34, 126.97, 126.40, 126.31, 121.63, 118.35, 116.37, 114.21, 112.45, 102.76, 94.65, 70.52, 67.26, 58.22, 51.40 (2C), 47.18, 32.11 (2C). HRMS (ESI+), calcd for $C_{31}H_{31}IN_5O_3$ [M+H$^+$]: m/z = 648.1466, found 648.1468.

*2.2.5. N-3-(tributylstannyl)-benzoyl-1-{2-[5-(2-methoxyethoxy)-1H-benzo[d]imidazol-1-yl]-quinolin-8-yl}-piperidin-4-amine (ATE-IQP) (**19**)*

The mixture of **12** (27 mg, 73.0 μmol, 1.0 eq.), DIPEA (15 μL, 80.0 μmol, 1.1 eq.), and **16** (40 mg, 80.0 μmol, 1.1 eq.) in dry dichloromethane (3 mL) was stirred at 50 °C for 3 h under nitrogen atmosphere. After completion of the reaction, the reaction mixture was diluted with dichloromethane and washed with water. The organic layer was dried over sodium sulfate, filtered, and concentrated under reduced pressure. The crude product purified by column chromatography on silica gel (chloroform/methanol = 100/1) to afford **19** (33 mg, 56%) as a pale yellow solid. ^{1}H-NMR (400 MHz, DMSO-d_6): δ 0.84 – 0.88 (9H, m), 1.01 – 1.18 (6H, m), 1.26 – 1.35 (6H, m), 1.45 – 1.60 (6H, m), 2.03 – 2.06 (4H, m), 2.86 – 2.91 (2H, m), 3.31 (3H, s), 3.66 – 3.72 (2H, m), 3.88 (2H, br d), 4.03 (1H, br s), 4.17 – 4.18 (2H, m), 7.30 – 7.38 (3H, m), 7.46 (1H, t, J = 7.2 Hz), 7.52 (1H, t, J = 8.0 Hz), 7.60 (1H, d, J = 7.6 Hz), 7.65 (1H, d, J = 7.2 Hz), 7.81 (1H, d, J = 8.0 Hz), 7.91 (1H, s), 8.18 (1H, d, J = 9.2 Hz), 8.51 (1H, d, J = 7.6 Hz), 8.56 (1H, d, J = 9.2 Hz), 8.92 (1H, d, J = 8.8 Hz), 9.19 (1H, s). ^{13}C NMR (100 MHz, DMSO-d_6): δ 166.56, 155.56, 149.08, 146.94, 145.12, 142.39, 141.39, 140.50, 140.31, 138.81, 135.13, 134.47, 127.60, 127.33, 126.94, 126.35, 126.29, 121.56, 118.27. 116.30, 114.26, 112.43, 102.68, 70.51, 67.21, 58.13, 51.40 (2C), 47.01, 32.21 (2C), 28.58 (3C), 26.68 (3C), 13.53 (3C), 9.21 (3C). HRMS (ESI+) calcd for $C_{43}H_{58}N_5O_3Sn$ [M+H$^+$]: m/z = 812.3556, found 812.3573).

2.3. Cell viability assays

TR-PCT1 cells were seeded on 96-well culture plates (5 x 10^3 cells/well) and cultured in DMEM medium containing 2% FBS and 20 ng/mL PDGF-BB at 33 °C in a humidified 5% CO_2 atmosphere. Cells were treated with each compound for 72 h

and cell viability was assessed using the Cell Counting Kit following the manufacturer's instructions. Briefly, cells were incubated with WST-8 at 33 °C in a humidified 5% CO_2 atmosphere for 30 min, followed by measuring optical density at 450 nm.

2.4. Radiolabeling

Radiotracers, [^{125}I]IIQP and [^{125}I]IB-IQP, were synthesized by an iododestannylation reaction of the corresponding tributylstannyl precursors (**15** or **19**) using NCS as an oxidizing agent. The radiotracers were isolated by RP-HPLC using a Cosmosil 5C_{18}MSII column (4.6 ID × 150 mm) at the flow rate of 1 mL/min with a gradient mobile phase of 70% methanol in water with 0.05% TEA to 90% methanol in water with 0.05% TEA for 20 min. The column temperature was maintained at 40 °C. Radiochemical yield and purity were determined by an auto well gamma counter.

*2.4.1. Synthesis of [^{125}I]IIQP (**20**)*

A solution of [^{125}I]NaI in 0.1 M NaOH aqueous solution (non-carrier added, 370 kBq, 2 μL) was charged into a sealed vial containing **5** (1 mg/mL, 5 μL), acetic acid (5%, 30 μL), acetonitrile (55 μL), and NCS (5 mg/mL, 10 μL). The mixture was shaken at room temperature for 15 min, quenched by addition of sodium hydrogensulfite (5 mg/mL, 10 μL) and the solvent was removed by nitrogen gassing. TFA was added to the residue and the shaking was allowed to continue for 30 min. After removing TFA by nitrogen gassing, the residue was mixed with initial mobile

phase of HPLC. The reaction mixture was shaken for some minutes, filtered, and analyzed by HPLC.

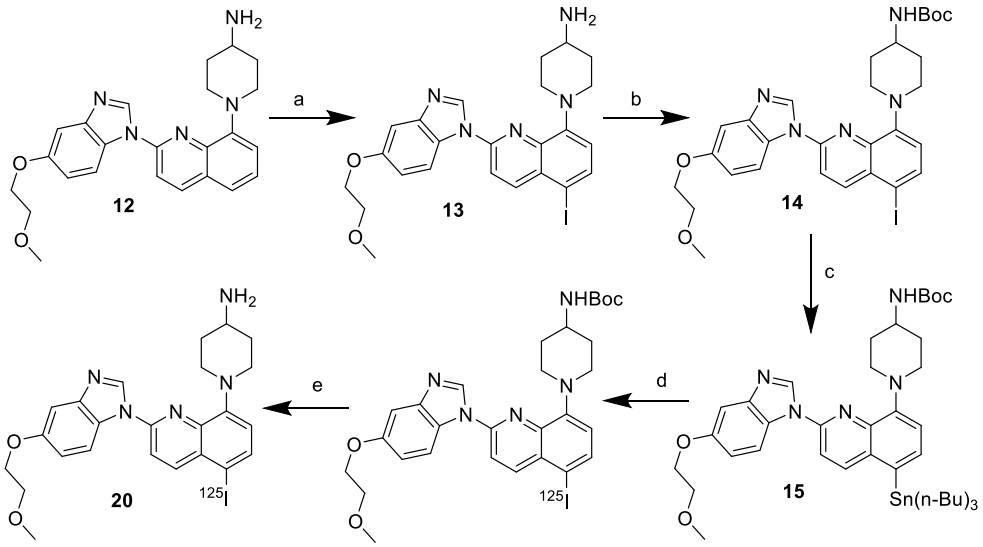

Scheme 2. Synthesis of reference compound, precursor, and radioiodinated compound [^{125}I]IIQP (a) NCS, NaI, 50 °C, 18 h (b) Boc_2O, TEA, room temperature, 3 d (c) hexabutyldistannane, $Pd[P(C_6H_5)_3]_4$, reflux, 24 h (d) [^{125}I]NaI, NCS, acetic acid, room temperature, 15 min (e) TFA, room temperature, 30 min.

*2.4.2. Synthesis of [^{125}I]IB-IQP (**21**)*

A solution of [^{125}I]NaI in 0.1 M NaOH aqueous solution (non-carrier added, 370 kBq, 2 µL) was added in a sealed vial containing **19** (1 mg/mL, 5 µL), acetic acid (5%, 10 µL), acetonitrile (10 µL), and NCS (5 mg/mL, 15 µL). The mixture was shaken at room temperature for 15 min, quenched by addition of sodium hydrogensulfite (5 mg/mL, 15 µL) and purified by HPLC.

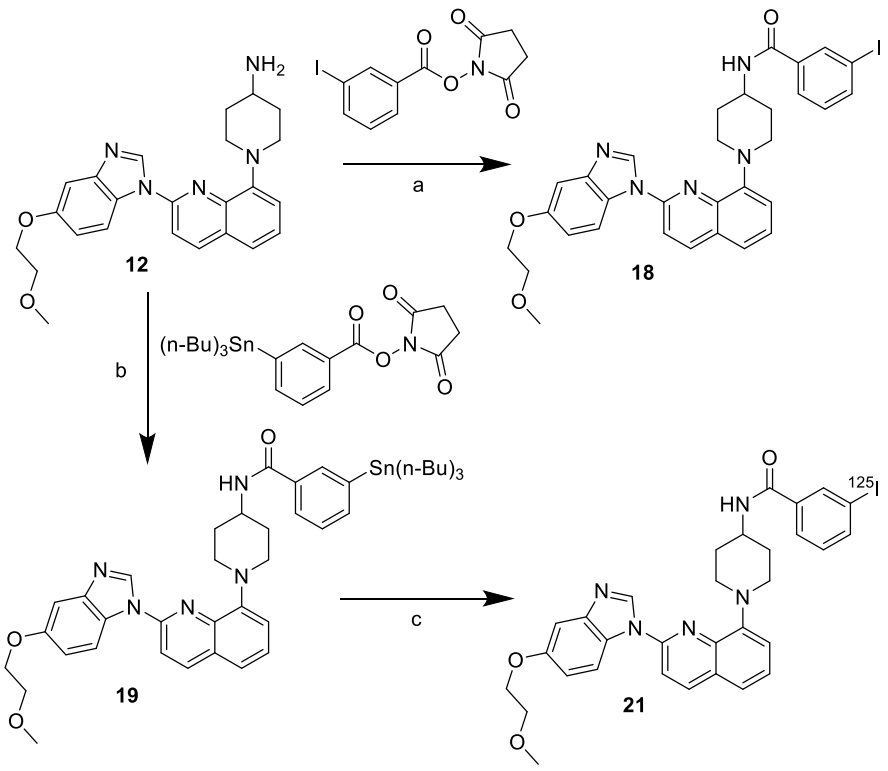

Scheme 3. Synthesis of reference compound, precursor, and radioiodinated compound [^{125}I]IB-IQP (a) 50 °C, 2 h; (b) 50 °C, 3 h; (c) [^{125}I]NaI, NCS, acetic acid, room temperature, 15 min.

2.5. Determination of partition coefficients

Partition coefficients of [^{125}I]IIQP and [^{125}I]IB-IQP into *n*-octanol and 0.1 M phosphate buffer (PB) pH 7.4 were measured as described previously with a slight modification.[38] Briefly, [^{125}I]IIQP or [^{125}I]IB-IQP was added to the mixture of *n*-octanol (3.0 mL) and PB (3.0 mL) in a test tube. The test tube was vortexed (1 min), left at room temperature (10 min), and centrifuged (5 min, 3,060*g*, 4 °C). *n*-Octanol layer (2.0 mL) was transferred into new test tube followed by addition of fresh *n*-octanol (1.0 mL) and PB (3.0 mL). After repeating vortex, standing, and centrifuge, radioactivity of each layer, *n*-octanol (1.0 mL) and PB (1.0 mL), was counted using an auto well gamma counter (n = 4).

2.6. In vitro stability assay

The stability of radiotracers, [^{125}I]IIQP and [^{125}I]IB-IQP, were analyzed as described previously with a slight modification.[39] Briefly, [^{125}I]IIQP or [^{125}I]IB-IQP solution (50 μL) in sealed tube containing 0.1 M phosphate buffered saline (PBS) pH 7.4 (450 μL) was incubated at 37 °C for 1, 3, 6, and 24 h. After incubation, the purities of radiotracers were analyzed by TLC using chloroform/methanol = 5/1 and 20/1 for [^{125}I]IIQP and [^{125}I]IB-IQP, respectively as a developing solvent and the results were confirmed by HPLC.

2.7. Cellular uptake study

BxPC3-luc or MCF7 cells were cultured in RPMI 1640 medium containing 10% FBS and penicillin (100 IU/mL)-streptomycin (100 μg/mL) on 6-well culture plates (containing 2 x 10^5 cells/well) for 24 h using a humidified atmosphere (5% CO_2) incubator at 37 °C. After removal of medium, a solution of [^{125}I]IIQP or [^{125}I]IB-IQP (3.7 kBq/well) in medium without FBS was added. After incubation for 0.5, 1, 2, and 4 h, the medium from each well was removed and the cells were washed once with ice-cold PBS (1 mL). The cells were dissolved using 1 M NaOH aqueous solution (0.5 mL) and wells were washed with 1 M NaOH aqueous solution (0.5 mL). The radioactivity of pooled basic fractions was determined using an auto well gamma counter. The total cell protein was quantified using a BCA Protein Assay Kit following the manufacturer's recommendations and bovine serum albumin as a protein standard. All data were expressed as percent dose per microgram protein (%dose/μg protein).

In blocking experiments, inhibitors (IQP, IIQP, or IB-IQP with final concentration 10 μM) in 1 mL of medium without FBS were added to wells containing 2 x 10^5 cells/well. After incubation for 10 min, [^{125}I]IIQP or [^{125}I]IB-IQP (3.7 kBq/well) in 1 mL of medium without FBS was added to each well. Radioactivity and protein concentration in cells were determined using the same method above-mentioned.

2.8. Competitive binding assay using BxPC3-luc cells

BxPC3-luc cells in RPMI 1640 medium containing 10% FBS and penicillin (100 IU/mL)-streptomycin (100 μg/mL) were seeded on 96-well plates (containing 5,000 cells/wells) and incubated for 24 h using a humidified atmosphere (5% CO_2) at 37 °C. [^{125}I]IIQP and nine concentrations (ranging from 1 pM to 1 mM) of displacing nonradiolabeled ligands (IQP, IIQP and IB-IQP) in assay buffer (25 mM HEPES, pH adjusted to 7.4) were added. After incubation at 37 °C for 90 min, the cells were washed twice with ice-cold PBS (150 μL) to remove the unbound radioligand. The cells were dissolved using 1 M NaOH aqueous solution (150 μL) and wells were washed with 1 M NaOH aqueous solution (150 μL). The bound radioactivity was determined using an auto well gamma counter. IC_{50} values were calculated by GraphPad Prism 5.0 software (La Jolla, CA, USA).

2.9. Animals

All animal handling procedures were approved by the Kanazawa University Animal Care Committee (Permit Number: AP-132633). Experiments with animals

were conducted in accordance with the Guidelines for the Care and Use of Laboratory Animals of Kanazawa University. The animals were housed with free access to food and water at 23 °C with a 12 h light/dark schedule. Six week-old male ddY (27 – 30 g) and four week-old female BALB/c *nu/nu* mice (12 – 17 g) were purchased from Japan SLC Inc. (Hamamatsu, Japan). For preparing tumor-bearing model, 5 x 10^6 BxPC3-luc cells were subcutaneously inoculated into left shoulder of BALB/c *nu/nu* mice. The tumor reached palpable size after 2 weeks of the inoculation.

2.9.1. Biodistribution study

A saline solution of [^{125}I]IIQP or [^{125}I]IB-IQP (74 kBq, 100 μL) containing 1% tween-80 and 10% ethanol was injected intravenously into the tail of the mice. The ddY mice were sacrificed at 2, 10 min, 1, 4, and 24 h, meanwhile the tumor-bearing mice were sacrificed at 1 h and 4 h ([^{125}I]IIQP) postinjection.

For *in vivo* blocking studies, female BALB/c *nu/nu* mice were intraperitoneally injected with IQP (40 mg/kg) as a blocking agent 1 h prior to intravenously injection of [^{125}I]IIQP (37 kBq, 100 μL). The mice were sacrificed at 1 h after administration of radiotracer.

Tissues of interest were removed and weighed. The radioactivity of the tissues was determined using an auto well gamma counter, and counts were corrected for background radiation. The data were expressed as percent injected dose per gram tissue (%ID/g).

2.10. Statistical analysis

All data were analyzed using GraphPad Prism 5.0 software and displayed as mean ± standard deviation (SD). Significance for *in vitro* blocking studies was calculated using a one-way analysis of variance (ANOVA) followed by Dunnett's post hoc test compared to the control group. Significance in cell viability assays was determined using ANOVA followed by Tukey's post hoc test. Significant differences of biodistribution in normal mice and tumor-bearing mice between [^{125}I]IIQP and [^{125}I]IB-IQP groups were determined using Student's *t*-test (unpaired, two-tailed). Significance for *in vivo* blocking studies between control and blocking groups were calculated using Student's *t*-test (unpaired, two-tailed). Results were considered statistically significant at $p < 0.05$.

3. Results

3.1. Synthesis of reference compounds and precursors

Lead compound **12** (Scheme 1) and the non-radioactive iodinated reference compounds, **13** and **18,** were easily obtained. Iodine was incorporated to the C-5 of quinoline core of IQP using mixture reagents of NCS and NaI with stirring at 50 °C for 18 h in acetic acid to obtain compound **13** (Scheme 2). On the other hand, compound **18** was synthesized by stirring the mixture of synthesized SIB and IQP at 50 °C for 2 h in a basic solution (Scheme 3). Retention time for compounds **13** and **18** on RP-HPLC were 11.7 and 12.5 min, respectively (Supporting Information). For synthesis of tin precursor **15**, utilizing the Pd(0) catalyst, tri-butyl tin group was introduced into IQP instead of iodine in **14** to obtain compound **15** in 48% yield after

purification using RP-HPLC. Meanwhile, compound **19** was obtained by the reaction between ATE and IQP with 56% yield.

3.2. Cell viability assays

To assess the binding potential of IIQP and IB-IQP to the ATP-binding site of PDGFRβ, TR-PCT1 cells were cultured in the presence of various concentration of IQP, IIQP, or IB-IQP (1 – 1000 nM). As displayed in Figure 2, the effects of IB-IQP were similar to those of IQP; however, IIQP was more effective than IQP in reducing the viability of TR-PCT1 cells.

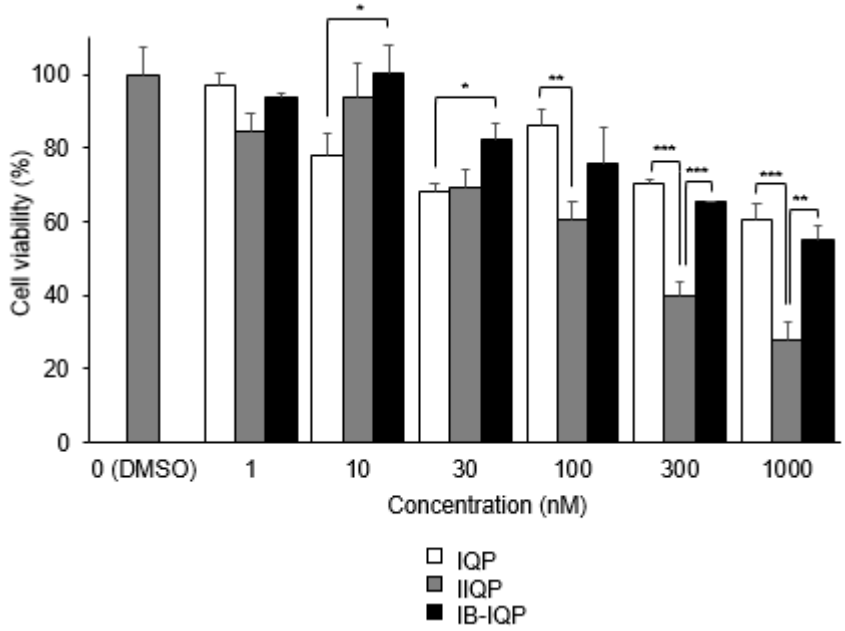

Figure 2. Cell viability after exposure to IQP, IIQP, and IB-IQP by WST-8 assay. Data are presented as mean ± SD for three samples. Significance was determined using a one-way ANOVA followed by Tukey's post hoc test ($^{*}p < 0.05$, $^{**}p < 0.01$, $^{***}p < 0.001$).

3.3. Radiolabeling

Two novel ^{125}I labeled IQP, [^{125}I]IIQP and [^{125}I]IB-IQP, were synthesized by an iododestannylation reaction with the corresponding tributyltin precursors, as outlined in Schemes 2 and 3, respectively. Both these radiotracers were synthesized using NCS

as an oxidizing agent in an acidic solution at room temperature in high radiochemical yield (95 and 85%, respectively). After purification using RP-HPLC, the radiochemical purities were over 99%.

3.4. Partition coefficient

The *n*-octanol/PB partition coefficients for [^{125}I]IIQP and [^{125}I]IB-IQP were 2.71 ± 0.03 and 3.19 ± 0.17, respectively. Lipophilicity of [^{125}I]IB-IQP was higher than that of [^{125}I]IIQP.

3.5. In vitro stability assay

The stability of radiotracers in 0.1 M PBS (pH 7.4) was evaluated using TLC analysis and confirmed using HPLC. After incubation for 24 h at 37 °C, the purity of the radiotracers remained high, and 93.9 ± 0.4% of [^{125}I]IIQP and 94.1 ± 0.7% of [^{125}I]IB-IQP remained intact.

3.6. Cell uptake study

The *in vitro* cell uptake experiments of [^{125}I]IIQP and [^{125}I]IB-IQP were performed using two types of cell lines: PDGFRβ-positive BxPC3-luc cells and PDGFRβ-negative MCF7 cells.[15,18,40] As shown in Figure 3, BxPC3-luc cells showed higher uptake of [^{125}I]IIQP and [^{125}I]IB-IQP then that by MCF7 cells. The uptake of [^{125}I]IIQP in BxPC3-luc cells reached 2.34 %dose/μg protein after 4 h incubation, whereas that of [^{125}I]IB-IQP reached 0.95 %dose/μg protein.

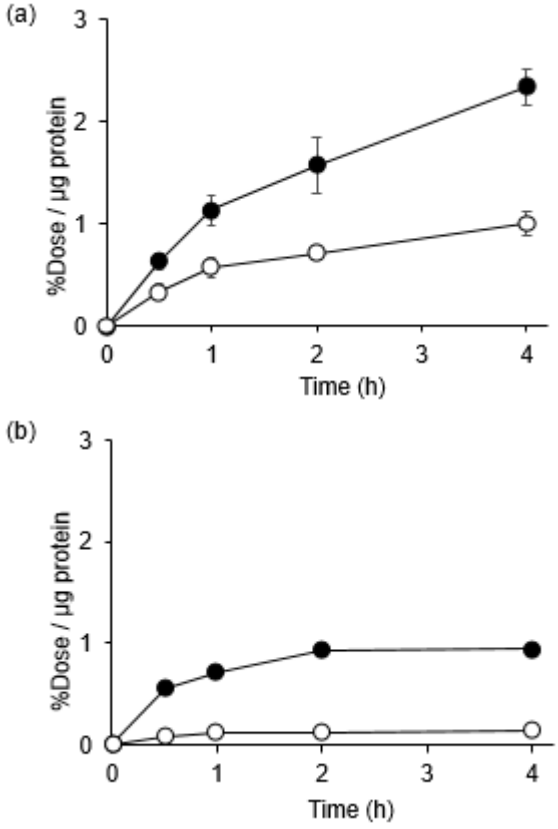

Figure 3. Cellular uptake study. Time-dependent accumulation of (a) [^{125}I]IIQP and (b) [^{125}I]IB-IQP in BxPC3-luc (closed circles) and MCF7 (open circles) cells. Data were presented as mean ± SD for three samples.

In the blocking studies, the uptakes of [^{125}I]IIQP and [^{125}I]IB-IQP in BxPC3-luc cells were significantly reduced by the pretreatment of excess amount of a PDGFRβ ligand, IQP, or non-radiolabeled compounds, IIQP or IB-IQP (Figure 4).

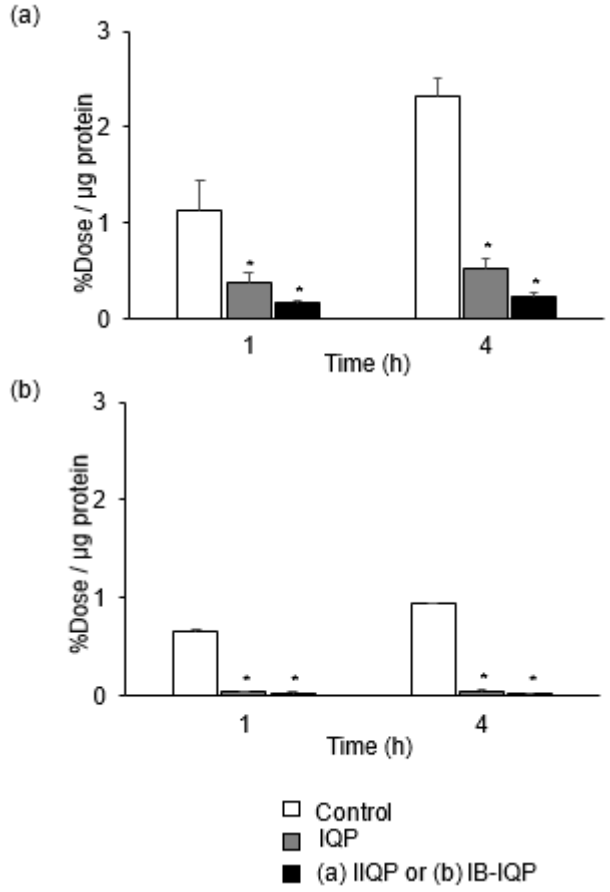

Figure 4. *In vitro* blocking study of (a) [^{125}I]IIQP and (b) [^{125}I]IB-IQP in BxPC3-luc cells. Data were presented as mean ± SD for three samples. Significance was determined using a one-way ANOVA followed by Dunnett's post hoc test ($^{*}p < 0.001$, vs control [^{125}I]IIQP or [^{125}I]IB-IQP).

3.7. Competitive binding assay using BxPC3-luc cells

The competitive binding of [^{125}I]IIQP to BxPC3-luc cells was investigated in the presence of PDGFRβ ligand, IQP, IIQP, and IB-IQP. The IC_{50} values were found to be 311 ± 82 nM for IQP, 44 ± 17 nM for IIQP, and 422 ± 54 nM for IB-IQP.

3.8. Biodistribution studies

Biodistribution of [^{125}I]IIQP and [^{125}I]IB-IQP in normal mice is summarized in Table 1. High accumulation of radioactivity after administration in liver, small intestine, and large intestine were shown. It was excreted into feces from these tissues during 24 h. It indicated that main excretion route of both [^{125}I]IIQP and [^{125}I]IB-IQP

was hepatobiliary. It was confirmed that the radioactivity in feces excreted during 24 h after injection of [^{125}I]IIQP and [^{125}I]IB-IQP (75.93 and 68.75 %ID, respectively) were much higher than the radioactivity in urine (3.79 and 13.48 %ID, respectively). Additionally, radioactivity was hardly observed in any tissues after 24 h evaluation for both radiotracers.

Biodistribution of [^{125}I]IIQP and [^{125}I]IB-IQP in BxPC3-luc tumor-bearing mice is summarized in Table 2. Accumulation of radioactivity in tumor at 1 h postinjection of [^{125}I]IIQP (1.29 %ID/gram) was significantly higher than that of [^{125}I]IB-IQP (0.52 %ID/gram) in biodistribution experiments using BxPC3-luc tumor-bearing mice. Accumulation of radioactivity in tumor at 4 h postinjection of [^{125}I]IIQP was 0.45 %ID/gram, which was lower than that at 1 h postinjection.

In *in vivo* blocking studies, the effect of IQP, a high affinity ligand for PDGFRβ, on tumor uptake of [^{125}I]IIQP at 1 h after administration is shown in Figure 5. In this case, the radioactivity level in the blood after injection of [^{125}I]IIQP was significantly increased by pretreatment of IQP. The values of % injected dose per gram of control group and IQP pretreatment group were 0.69 ± 0.10 and 3.16 ± 0.15, respectively. Thus, the figures are shown as not only % injected dose per gram but also as tumor / blood ratio. The result demonstrated that pretreatment of an excess amount of IQP resulted in a significant decrease in tumor uptake and the uptake ratio of tumor to blood at 1 h postinjection of [^{125}I]IIQP.

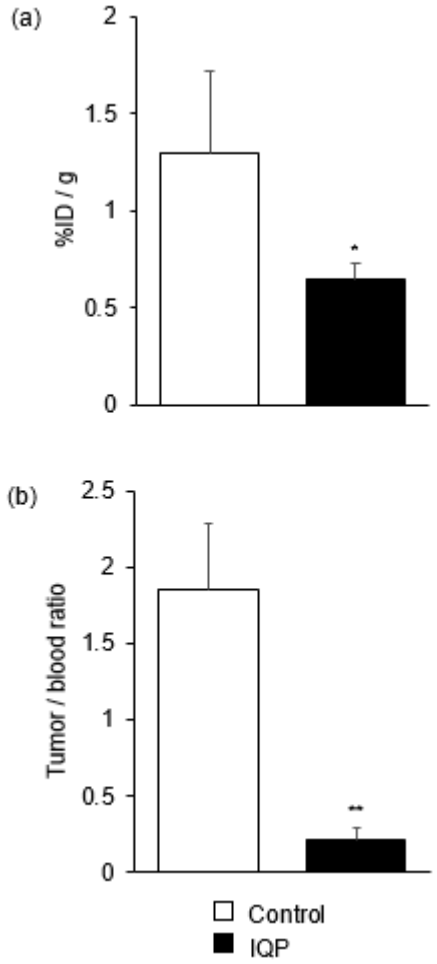

Figure 5. Tumor uptake and tumor/blood uptake ratios of [^{125}I]IIQP at 1 h postinjection with IQP (40 mg/kg) (blocking group) or control group. Data were presented as means ± SD for three or four mice. Significance was determined using an unpaired Student's *t*-test ($^{*}p < 0.05$, $^{**}p < 0.001$).

4. Discussion

To develop probes for PDGFRβ imaging, the affinity of newly synthesized IQP analogs, which contain iodine molecules, for PDGFRβ, was evaluated using WST-8 assay. WST-8 assay determines cell viability; therefore, it cannot directly be used for affinity studies. A negative correlation is speculated between the PDGFRβ-analog affinity and TR-PCT1 cell viability because TR-PCT1 cells express PDGFRβ, and they die when the receptor signaling pathway is interrupted.[41,42] Therefore, WST-8 assay was used as an index to evaluate affinity changes between the ligand and PDGFRβ by introducing an iodine molecule in IQP. IB-IQP and IQP displayed similar

affinity for PDGFRβ as a molecular target, whereas IIQP displayed a higher affinity than that of IQP (Figure 2). A competitive binding assay was also performed to evaluate the affinity of ligands for PDGFRβ. The competitive binding of [^{125}I]IIQP to BxPC3-luc cells was investigated in the presence of PDGFRβ ligands, IQP, IIQP, and IB-IQP. In this assay, [^{125}I]IIQP do not always bind to only PDGFRβ in tumor cells. Thus, the IC_{50} values of the experiments may not indicate the affinity for PDGFRβ completely. However, the IC_{50} values should be an index of the affinity. As the results, the IC_{50} value of IIQP (44 nM) was lower than those of IQP (311 nM) and IB-IQP (422 nM), indicating that IIQP possesses higher affinity than IQP and IB-IQP. It was consistent with WST-8 assay. Generally, the introduction of certain molecules, functional groups or elements into lead compounds can reduce their affinity for target molecules. However, in this study, the introduction of iodine into IQP increased the affinity of IIQP for PDGFRβ. This result is extremely favorable for developing molecular probes for PDGFRβ imaging.

Iodogen, chloramine-T (CAT), NCS, and peracetic acid (PAA) are commonly used as oxidizing agents for the preparation of radioiodinated compounds. [^{125}I]IIQP and [^{125}I]IB-IQP were synthesized using an iododestannylation technique without the addition of a carrier and using NCS as an oxidizing agent with excellent radiochemical yields. We also tried to synthesize [^{125}I]IIQP and [^{125}I]IB-IQP using CAT and PAA as oxidizing agents; however, the radiochemical yields were <50%. These results indicated that NCS is the most suitable oxidizing agent for compounds with oligo arene, such as IIQP and IB-IQP.

In cellular uptake experiments for [^{125}I]IIQP and [^{125}I]IB-IQP, these radiotracers showed higher accumulation in PDGFRβ-positive tumor cells (BxPC3-luc) than in PDGFRβ-negative tumor cells (MCF7). [^{125}I]IIQP, which had the highest affinity for PDGFRβ in the competitive binding assay and WST-8 assay, showed higher accumulation in PDGFRβ-positive tumor cells than that of [^{125}I]IB-IQP (Figure 3). In *in vivo* experiments, [^{125}I]IIQP showed significantly higher accumulation in BxPC3-luc tumor than that of [^{125}I]IB-IQP (Table 2). Moreover, the uptake of [^{125}I]IIQP in PDGFRβ-positive tumor cells was inhibited by treatment with an excess amount of PDGFRβ ligand both in the cellular uptake study (Figure 4) and in the *in vivo* blocking experiments using tumor-bearing mice (Figure 5). These results indicated that the uptake of [^{125}I]IIQP in tumors is PDGFRβ-specific, and it must bind the ATP-binding site of PDGFRβ in the tumor cell.

Small molecule TKIs, including [^{125}I]IIQP and [^{125}I]IB-IQP, target the intracellular domain of RTKs, and for this binding, they should diffuse through the cellular membrane. The log *P* values of the compounds are an important factor to penetrate the cellular membrane. It has been shown that a log *P* value of 1 to 3.5 is required to passively penetrate cellular membrane.[43-46] In this study, Log *P* values of [^{125}I]IIQP and [^{125}I]IB-IQP were 2.71 and 3.19, respectively. This suggested that the lipophilicity of both the radiotracers was suitable for them to be used as PDGFRβ imaging probes.

In the biodistribution experiments, [^{125}I]IIQP and [^{125}I]IB-IQP were mainly excreted through the hepatobiliary pathway, which is often observed for small molecule radiotracers directed to the ATP-binding site of TKs.[20,23,47,48] This excretion

route may be due to the moderately high lipophilicities of these radiotracers. Meanwhile, it has been known that free iodine accumulates in the stomach and thyroid; this is used as an index of deiodination of radioiodine-labeled tracers *in vivo*. In this study, the accumulation in the stomach was not high, suggesting that both [^{125}I]IIQP and [^{125}I]IB-IQP are highly stable not only *in vitro* but also *in vivo*. In the case of [^{125}I]IIQP, the biodistribution study in tumor-bearing mice at 4 h postinjection was performed because we expected more effective tumor detection derived from higher accumulation ratios of tumor / non-target tissues. The results showed that the tumor accumulation decreased; however, tumor to blood and tumor to muscle ratios at 4 h postinjection were higher than those at 1 h postinjection because radioactivity in the blood and muscle was prominently decreased. Many studies have reported that P glycoprotein (P-gp), breast cancer resistant protein (BCRP), and/or other drug efflux transporters can hinder tumor uptake of anticancer drugs.[49,50] Planar structure, high lipophilicity, and neutral or positive charges are some of requirements for P-gp substrates.[51] Because [^{125}I]IIQP possesses these characteristics, it can be a substrate for P-gp and therefore, its accumulation may have decreased in tumor cells. However, further research is warranted to prove whether [^{125}I]IIQP is a P-gp substrate. Another possibility is the presence of radioactive metabolites that have less or no affinity to the molecular target. Rapid metabolism leads to the loss of affinity for target molecules and resulting low tumor uptake.[52] Although [^{125}I]IIQP showed high stability both *in vitro* and *in vivo*, this possibility cannot be completely excluded because we did not perform a metabolic study.

5. Conclusion

In this study, we synthesized the radiolabeled compounds [^{125}I]IIQP and [^{125}I]IB-IQP using an iododestannylation reaction under non-carrier added condition with high radiochemical yields and high purities. This method can also be used to synthesize other radioiodinated compounds containing quinoline-benzimidazole derivatives. The present study showed that radioiodinated IIQP could be a promising imaging agent compared with radioiodinated IB-IQP. However, modification of its structure may be needed to obtain appropriate PDGFRβ-targeted imaging agents, which have higher tumor uptake and tumor to background ratios.

6. Acknowledgments

This work was supported in part by Grants-in-Aid for Scientific Research (16H01332, 16KT0192) from the Ministry of Education, Culture, Sports, Science and Technology, Japan.

References

1. Yu, J.; Ustach, C.; Kim, H. R. C. *J. Biochem Mol Biol.* **2003**, *36,* 49-59.
2. Criscitiello, C.; Gelao, L.; Viale, G.; Esposito, A.; Curigliano, G. *Expert Opin Investig Drugs.* **2014**, *23,* 599-610.
3. Östman, A.; Heldin, C. H. *Adv Cancer Res* **2007**, *97,* 247-274
4. Levitzki, A.; Gazit, A. *Science.* **1995**, *267,* 1782-1788.
5. Östman, A. *Cytokine Growth Factor Rev.* **2004**, *15,* 275-286.
6. Lindborg, M.; Cortez, E.; Höidén-Guthenberg, I.; Gunneriusson, E.; von Hage, E.; Syud, F.; Morrison, M.; Abrahmsén, L.; Herne, N.; Pietras, K.; Frejd, F. Y. *J Mol Biol*. **2011**, *407,* 298-315.
7. Pietras, K.; Sjöblom, T.; Rubin, K.; Heldin, C. H.; Östman, A. *Cancer Cell.* **2003**, *3,* 439-443.
8. Benezra, M.; Hambardzumyan, D.; Penate-Medina, O.; Veach, D. R.; Pillarsetty, N.; Smith-Jones, P.; Phillips, E.; Ozawa, T.; Zanzonico, P. B.; Longo, V.; Holland, E. C.; Larson, S. M.; Bradbury, M. S. *Neoplasia*. **2012**, *14,* 1132-1143.
9. Cornelissen, B. *J Labelled Comp Radiopharm.* **2014**, *57,* 310-316.
10. Fass, L. *Mol Oncol.* **2008**, *2,* 115-152
11. Cunha, L.; Szigeti, K.; Mathé, D.; Metello, L. F. *Drug Discov Today*. **2014**, *19,* 936-948.
12. Poot, A. J.; Slobbe, P.; Hendrikse, N. H.; Windhorst, A. D.; van Dongen, G. A. *Clin Pharmacol Ther.* **2013**, 93, 239-241.
13. Fretto, L. J.; Snape, A. J.; Tomlinson, J. E.; Seroogy, J. J.; Wolf, D. L.; LaRochelle, W. J.; Giese, N. A. *J Biol Chem*. **1993**, *268,* 3625-3631.
14. Maudsley, S.; Zamah, A. M.; Rahman, N.; Blitzer, J. T.; Luttrell, L. M.; Lefkowitz, R. J.; Hall, R. A. *Mol Cell Biol.* **2000**, *20,* 8352-8363.
15. Camorani, S.; Esposito, C. L.; Rienzo, A.; Catuogno, S.; Iaboni, M,; Condorelli, G.; de Franciscis, V.; Cerchia, L. *Mol Ther.* **2014**, *22,* 828-841.

16. Tolmachev, V.; Varasteh, Z.; Honarvar, H.; Hosseinimehr, S. J.; Eriksson, O.; Jonasson, P.; Frejd, F. Y.; Abrahmsen, L.; Orlova, A. *J Nucl Med.* **2014**, *55,* 294-300.
17. Strand, J.; Varasteh, Z.; Eriksson, O.; Abrahmsen, L.; Orlova, A.; Tolmachev, V. *Mol Pharm.* **2014**, *11,* 3957-3964.
18. Askoxylakis, V.; Marr, A.; Altmann, A.; Markert, A.; Mier, W.; Debus, J.; Huber, P. E.; Haberkorn, U. *Mol Imaging Biol.* **2013**, *15,* 212-221.
19. Marr, A.; Nissen, F.; Maisch, D.; Altmann, A.; Rana, S.; Debus, J.; Huber, P. E.; Haberkorn, U.; Askoxylakis, V. *Mol Imaging Biol.* **2013**, *15,* 391-400.
20. Yoshimoto, M.; Hirata, M.; Kanai, Y.; Naka, S.; Nishii, R.; Kagawa, S.; Kawai, K.; Ohmomo, Y. *Biol Pharm Bull.* **2014**, *37,* 355-360.
21. Yeh, H. H.; Ogawa, K.; Balatoni, J.; Mukhapadhyay, U.; Pal, A.; Gonzalez-Lepera, C.; Shavrin, A.; Soghomonyan, S.; Flores, L. II.; Young, D.; Volgin, A. Y.; Najjar, A. M.; Krasnykh, V.; Tong, W.; Alauddin, M. M.; Gelovani, J. G. *Proc Natl Acad Sci U S A.* **2011**, *108,* 1603-1608.
22. Fernandes, C.; Oliveira, C.; Gano, L.; Bourkoula, A.; Pirmettis, I.; Santos, I. *Bioorg Med Chem.* **2007**, *15,* 3974-3980.
23. Hirata, M.; Kanai, Y.; Naka, S.; Yoshimoto, M.; Kagawa, S.; Matsumuro, K.; Katsuma, H.; Yamaguchi, H.; Magata, Y.; Ohmomo, Y. *Ann Nucl Med.* **2013**, *27,* 431-443.
24. Kuchar, M.; Oliveira, M. C.; Gano, L.; Santos, I.; Kniess, T. *Bioorg Med Chem Lett.* **2012**, *22,* 2850-2855.
25. Wang, J. Q.; Miller, K. D.; Sledge, G. W.; Zheng, Q. H. *Bioorg Med Chem Lett.* **2005**, *15,* 4380-4384.
26. Wang, J. Q.; Gao, M.; Miller, K. D.; Sledge, G. W.; Zheng, Q. H. *Bioorg Med Chem Lett.* **2006**, *16,* 4102-4106.

27. Galbán, C. J.; Galbán, S.; Van Dort, M. E.; Luker, G. D.; Bhojani, M. S.; Rehemtulla, A.; Ross, B. D. *Prog Mol Biol Transl Sci*. **2010**, *95,* 237-398.
28. Tolmachev, V.; Stone-Elander, S.; Orlova, A. *Lancet Oncol.* **2010**, *11,* 992-1000.
29. Roberts, W. G.; Whalen, P. M.; Soderstrom, E.; Moraski, G.; Lyssikatos, J. P.; Wang, H. F.; Cooper, B.; Baker, D. A.; Savage, D.; Dalvie, D.; Atherton, J. A.; Ralston, S.; Szewc, R.; Kath, J. C.; Lin, J.; Soderstrom, C.; Tkalcevic, G.; Cohen, B. D.; Pollack, V.; Barth, W.; Hungerford, W.; Ung, E. *Cancer Res.* **2005**, *65,* 957-966.
30. Xi, Y.; Chen, M.; Liu, X.; Lu, Z.; Ding, Y.; Li, D. *Onco Targets Ther.* **2014**, *7,* 1215-1221.
31. Asashima, T.; Iizasa, H.; Terasaki, T.; Hosoya, K.; Tetsuka, K.; Ueda, M.; Obinata, M.; Nakashima, E. *Eur J Cell Biol.* **2002**, *81,* 145-152.
32. Weichert, D.; Banerjee, A.; Hiller, C.; Kling, R. C.; Hübner, H.;, Gmeiner, P. *J Med Chem.* **2015**, *58,* 2703-2717.
33. Sundriyal, S.; Malmquist, N. A.; Caron, J.; Blundell, S.; Liu, F.; Chen, X.; Srimongkolpithak, N.; Jin, J.; Charman, S. A.; Scherf, A.; Fuchter, M. J. *ChemMedChem.* **2014**, *9,* 2360-2373.
34. Zalutsky, M. R.; Narula, A. S. *Int J Rad Appl Instrum A*. **1987**, *38,* 1051-1055.
35. Arano, Y.; Wakisaka, K.; Ohmomo, Y.; Uezono, T.; Mukai, T.; Motonari, H.; Shiono, H.; Sakahara, H.; Konishi, J.; Tanaka, C.; Yokoyama, A. *J Med Chem.* **1994**, *37,* 2609-2618.
36. Barth, W.; Luzzio, M.; Lyssikatos, J. European Patent EP 1 235 825 B1, 2006, 1-136.
37. Niihama, K. Jpn. Kokai Tokkyo Koho Patent JP 2008031067, 2008.
38. Ogawa, K., Shiba, K.; Akhter, N.; Yoshimoto, M.; Washiyama, K.; Kinuya, S.; Kawai, K.; Mori, H. *Cancer Sci.* **2009**, *100,* 2188-2192.

39. Ogawa, K.; Kanbara, H.; Kiyono, Y.; Kitamura, Y.; Kiwada, T.; Kozaka, T.; Kitamura, M.; Mori, T.; Shiba, K.; Odani, A. *Nucl Med Biol.* **2013**, *40,* 445-450.

40. Chung, H.W.; Wen, J.; Lim, J. B.; Bang, S.; Park, S. W.; Song, S. Y. *Int J Radiat Oncol Biol Phys.* **2009**. *75*, 862-869.

41. Riese, D. J. *Expert Opin Drug Discov.* **2011**, *6,* 185-193

42. Weisberg, E.; Manley, P.; Mestan, J.; Cowan-Jacob, S.; Ray, A.; Griffin, J. D. *Br J Cancer*. **2006**, *94,* 1765-1769.

43. Waterhouse, R. N. *Mol Imaging Biol.* **2003**, *5,* 376-389.

44. Pike, V. W. *Trends Pharmacol Sci.* **2009**, 30, 431-440.

45. Dishino, D.D.; Welch, M. J.; Kilbourn, M. R.; Raichle, M. E. *J Nucl Med.* **1983**, *24,* 1030-1038.

46. VanBrocklin, H. F.; Lim, J. K.; Coffing, S. L.; Hom, D. L.; Negash, K.; Ono, M. Y.; Gilmore, J. L.; Bryant, I.; Riese, D. J. II. *J Med Chem.* **2005**, *48,* 7445-7456.

47. Zhang, M. R.; Kumata, K.; Hatori, A.; Takai, N.; Toyohara, J.; Yamasaki, T.; Yanamoto, K.; Yui, J.; Kawamura, K.; Koike, S.; Ando, K.; Suzuki, K. *Mol Imaging Biol.* **2010**, *12,* 181-191.

48. Samén, E.; Arnberg, F.; Lu, L.; Olofsson, M. H.; Tegnebratt, T.; Thorell, J. O.; Holmin, S.; Stone-Elander, S. *J Nucl Med.* **2013**, *54,* 1804-1811.

49. Asakawa, C.; Ogawa, M.; Kumata, K.; Fujinaga, M.; Kato, K.; Yamasaki, T.; Yui, J.; Kawamura, K.; Hatori, A.; Fukumura, T.; Zhang, M. R. *Bioorg Med Chem Lett.* **2011**, *21,* 2220-2223.

50. Chen, Y.; Agarwal, S.; Shaik, N. M.; Chen, C.; Yang, Z.; Elmquist, W. F. *J Pharmacol Exp Ther.* **2009**, *330,* 956-963.

51. Ogushi, N.; Sasaki, K.; Shimoda, M. *J Vet Med Sci.* **2017**, *79,* 320-327.

52. Slobbe, P.; Poot, A. J.; Haumann, R.; Schuit, R. C.; Windhorst, A. D.: van Dongen, G. A. *Nucl Med Biol.* **2016**, *43,* 612-624.

Table 1. Biodistribution of [^{125}I]IIQP and [^{125}I]IB-IQP at 2, 10 min, 1, 4, and 24 h after i.v. injection in ddY mice.

Tissues	Time after injection				
	2 min	10 min	1 h	4 h	24 h
[^{125}I]IIQP					
Blood	3.54 (0.21)	1.05 (0.15)	0.32 (0.03)	0.11 (0.01)	0.02 (0.02)
Liver	13.28 (1.16)	10.29 (0.86)	3.60 (0.59)	1.49 (0.42)	0.25 (0.04)
Kidney	14.85 (0.28)	15.09 (1.41)	9.54 (1.40)	3.55 (0.93)	0.16 (0.04)
Small intestine	2.91 (0.13)	11.19 (1.40)	28.53 (2.30)	6.89 (1.52)	0.06 (0.01)
Large intestine	0.84 (0.07)	0.75 (0.07)	1.59 (0.33)	52.43 (1.70)	0.17 (0.05)
Spleen	6.78 (0.96)	4.79 (0.49)	1.28 (0.13)	0.28 (0.09)	0.03 (0.00)
Pancreas	5.46 (0.41)	3.81 (0.41)	2.45 (0.24)	1.09 (0.13)	0.03 (0.01)
Lung	23.65 (1.45)	9.81 (1.54)	6.66 (2.29)	2.87 (0.54)	0.09 (0.00)
Heart	10.14 (0.75)	3.98 (0.28)	0.78 (0.11)	0.22 (0.01)	0.03 (0.00)
Stomach†	1.11 (0.16)	1.30 (0.09)	1.45 (0.29)	1.09 (0.20)	0.09 (0.03)
Bone	2.21 (0.29)	1.36 (0.15)	0.73 (0.05)	0.11 (0.00)	0.05 (0.01)
Muscle	3.46 (0.42)	1.96 (0.26)	0.65 (0.12)	0.18 (0.02)	0.01 (0.00)
Brain	0.19 (0.02)	0.06 (0.00)	0.03 (0.00)	0.02 (0.00)	0.00 (0.00)
Urine					3.79 (0.71)
Feces					75.93 (4.13)
[^{125}I]IB-IQP					
Blood	2.18 (0.22)**	1.15 (0.17)	0.29 (0.03)	0.07 (0.01)**	0.02 (0.00)
Liver	21.11 (1.02)**	18.99 (1.32)**	3.93 (0.38)	0.57 (0.06)**	0.07 (0.00)**
Kidney	9.30 (1.15)**	5.67 (0.73)**	1.48 (0.45)**	0.39 (0.06)**	0.04 (0.00)**
Small intestine	2.72 (0.40)	11.55 (3.07)	31.10 (2.25)	0.72 (0.10)**	0.01 (0.00)**
Large intestine	0.75 (0.02)	0.95 (0.04)**	1.20 (0.25)	16.53 (3.01)**	0.07 (0.00)*
Spleen	3.25 (0.47)**	2.09 (0.33)**	0.51 (0.05)**	0.09 (0.01)**	0.01 (0.00)**
Pancreas	3.64 (0.37)**	2.71 (0.54)*	0.94 (0.15)**	0.16 (0.01)**	0.00 (0.00)*
Lung	4.98 (1.83)**	2.02 (0.28)**	1.15 (0.25)**	0.63 (0.05)**	0.03 (0.01)**
Heart	5.95 (0.44)**	1.84 (0.30)**	0.50 (0.04)**	0.09 (0.01)**	0.00 (0.00)**
Stomach†	0.92 (0.03)	2.03 (0.89)	1.65 (0.38)	0.19 (0.09)**	0.01 (0.00)**
Bone	1.52 (0.26)*	0.81 (0.16)**	0.31 (0.04)**	0.06 (0.01)**	0.00 (0.00)**
Muscle	1.89 (0.37)**	1.09 (0.15)**	0.33 (0.01)**	0.08 (0.03)**	0.01 (0.00)
Brain	0.30 (0.06)*	0.20 (0.04)**	0.05 (0.00)*	0.02 (0.00)	0.00 (0.00)
Urine					13.48 (0.43)**
Feces					68.75 (6.44)

Data were presented as %injected dose / gram tissue. Each value represent mean ± SD for three or four mice. Significance was determined using an unpaired Student's *t*-test ($^{*}p < 0.05$, $^{**}p < 0.01$ vs. [^{125}I]IIQP).

† presented as %ID/organ.

Table 2. Biodistribution of [^{125}I]IIQP and [^{125}I]IB-IQP at 1 h and 4 h after i.v. injection in BxPC3-luc tumor-bearing mice.

Tissues	[^{125}I]IIQP		[^{125}I]IB-IQP
	1 h	4 h	1 h
Blood	0.69 (0.10)	0.15 (0.01)	0.23 (0.03)**
Liver	11.10 (2.64)	1.48 (0.10)	4.81 (0.66)*
Kidney	15.60 (2.05)	2.65 (0.37)	1.13 (0.09)**
Small intestine	37.37 (3.11)	3.98 (0.44)	45.53 (2.53)*
Large intestine	3.98 (1.35)	22.09 (2.87)	7.88 (3.74)
Spleen	3.46 (0.45)	0.35 (0.09)	0.61 (0.06)**
Pancreas	7.67 (2.50)	2.20 (0.20)	1.23 (0.16)*
Lung	12.28 (0.94)	2.73 (0.44)	1.16 (0.23)**
Heart	1.37 (0.13)	0.29 (0.07)	0.44 (0.02)**
Stomach†	2.99 (1.09)	0.20 (0.03)	0.26 (0.06)*
Bone	1.37 (0.13)	0.03 (0.05)	0.29 (0.03)**
Muscle	1.14 (0.25)	0.13 (0.01)	0.38 (0.03)**
Brain	0.14 (0.02)	0.03 (0.00)	0.05 (0.00)**
BxPC3-luc tumor	1.29 (0.43)	0.45 (0.04)	0.52 (0.09)*

Data were presented as means ± SD of %injected dose / gram of tissue for three or four mice. Significance was determined using an unpaired Student's *t*-test ($^{*}p < 0.05$, $^{**}p < 0.01$ vs. [^{125}I]IIQP).
† presented as %ID/organ.